Tuning the Current Rectification Behavior of Rh$_2$-Based Molecular Junctions by Variation of Supramolecular Structures

Donglei Bu#*, Changgeng Huang#, Pengzhan Sha, Shangxian Chen, Duocheng Bu, Shaoming Huang*

Authors contribute equally

School of Materials and Energy, Guangzhou Key Laboratory of Low-Dimensional Materials and Energy Storage Devices, Guangdong University of Technology, Guangzhou 510006, P. R. China
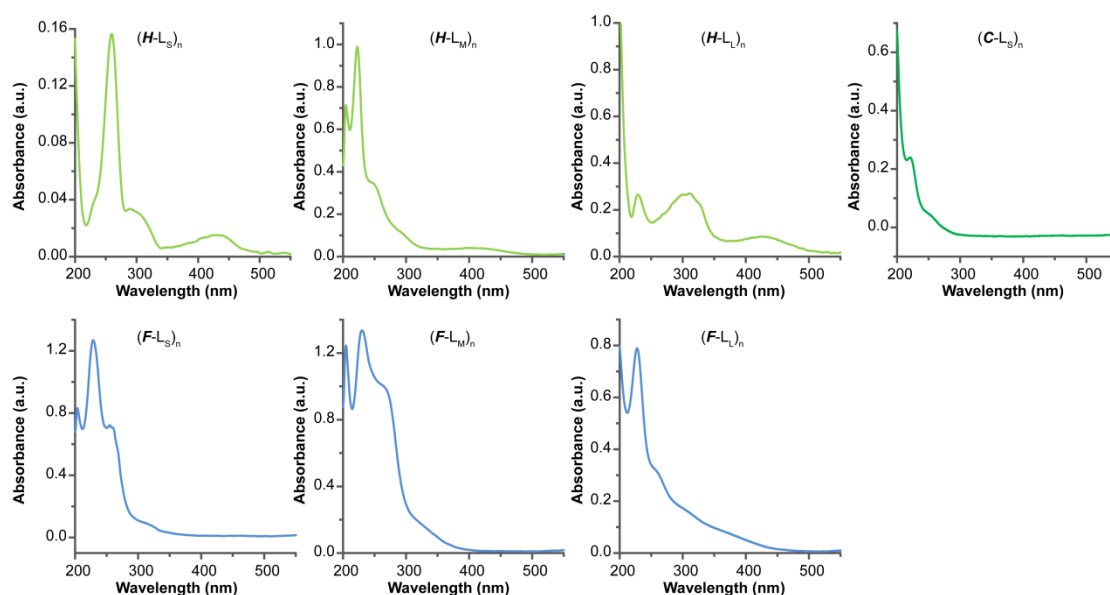
Figure S1. UV-vis spectra of (H-L$_S$)$_n$, (H-L$_M$)$_n$, (H-L$_L$)$_n$, (C-L$_S$)$_n$, (F-L$_S$)$_n$, (F-L$_M$)$_n$, and (F-L$_L$)$_n$ oligomers.
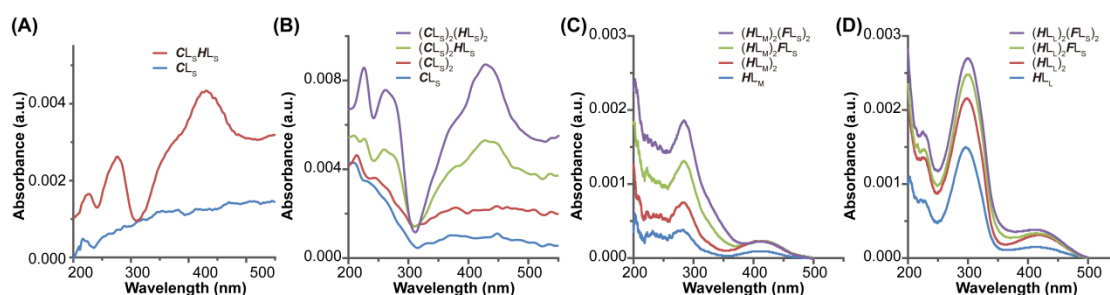
Figure S2. UV-vis spectroscopy monitoring the fabrication processes of the (A) CL$_S$$HL_S$, (B) ($CL_S$)$_2$($HL_S$)$_2$, (C) ($HL_M$)$_2$($FL_M$)$_2$, and (D) ($HL_L$)$_2$($FL_L$)$_2$ SAMs, respectively.
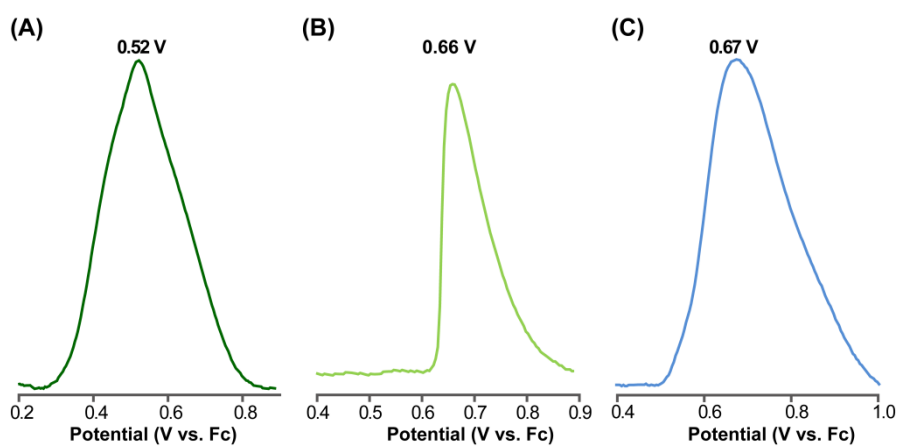
Figure S3. DPV of (A) (CL$_S$)$_n$, (B) (HL$_S$)$_n$, and (C) (FL$_S$)$_n$ oligomer, respectively.
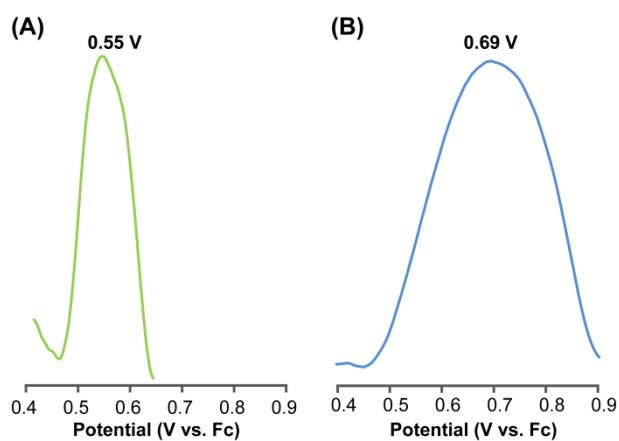

Figure S4. DPV of (A) (HL$_M$)$_n$, (B) and (FL$_M$)$_n$ oligomer, respectively.
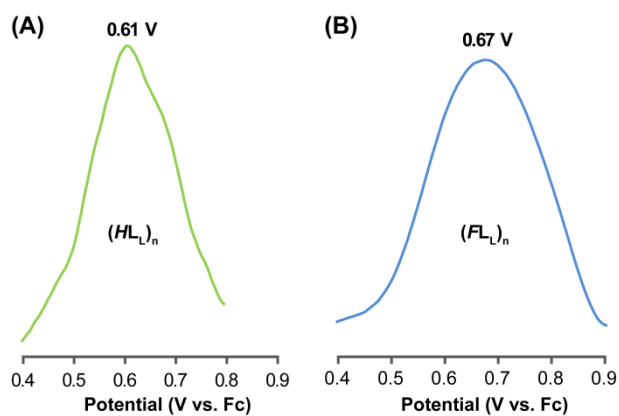

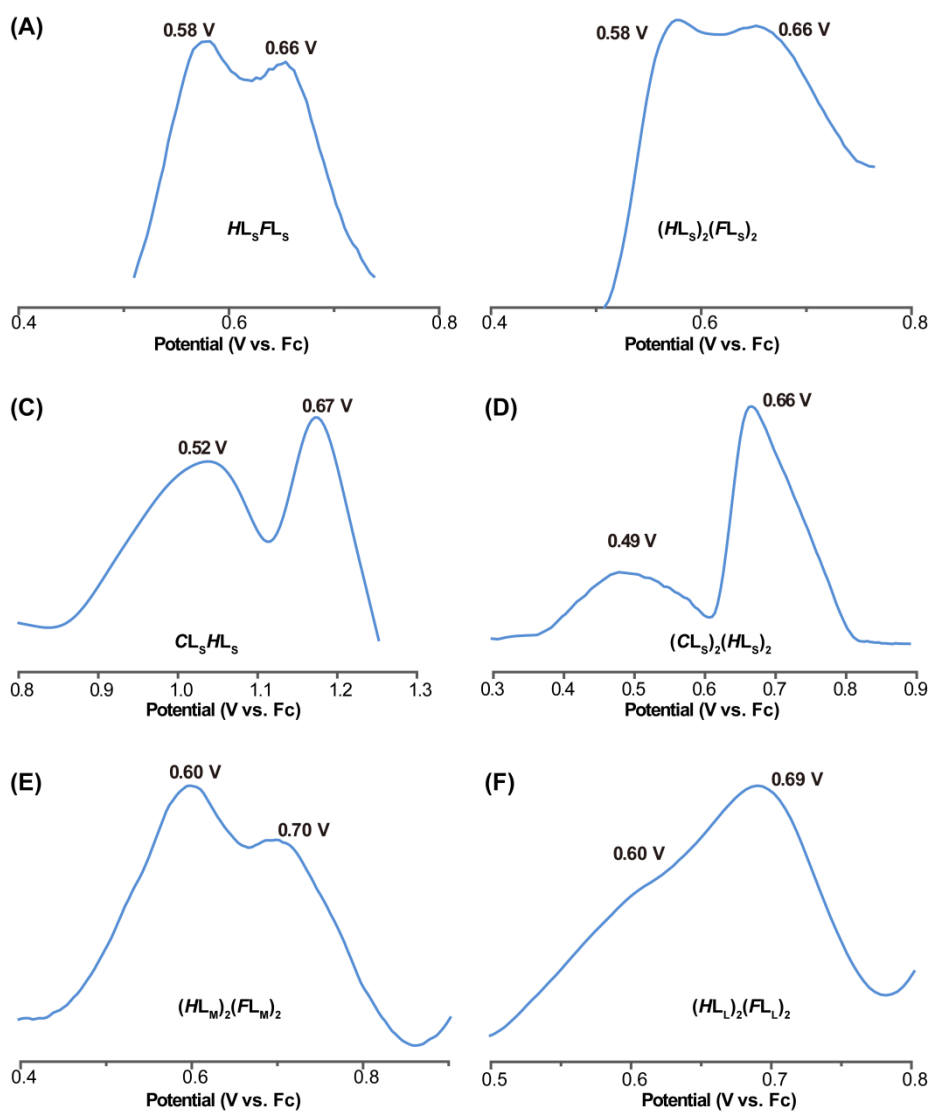Figure S5. DPV of (A) (HL$_L$)$_n$, (B) and (FL$_L$)$_n$ oligomer, respectively.

Figure S6. Electrochemical DPVs of (A)HL_SFL_S, (B) $(HL_S)_2(FL_S)_2$, (C) CL_SHL_S, (D) $(CL_S)_2(HL_S)_2$, (E) $(HL_M)_2(FL_M)_2$, and (F) $(HL_L)_2(FL_L)_2$, respectively.
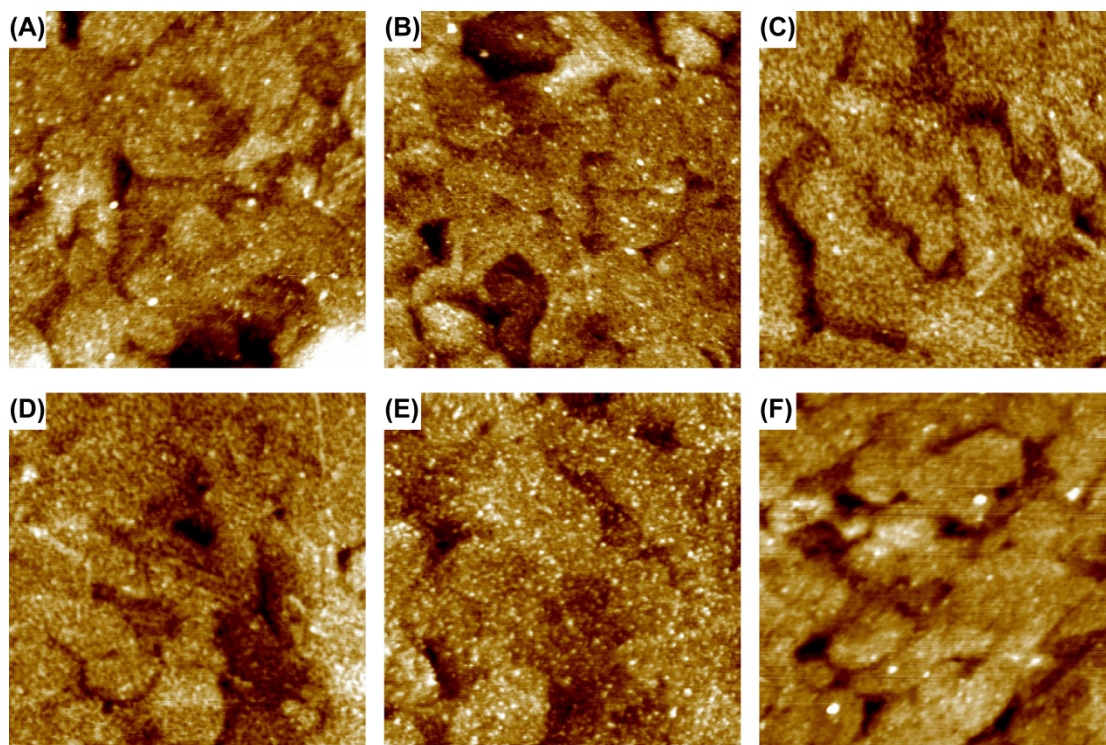
Figure S7. AFM topographic images of (A) HL_SFL_S, (B) $(HL_S)_2(FL_S)_2$, (C) CL_SHL_S, (D) $(CL_S)_2(HL_S)_2$, (E) $(HL_M)_2(FL_M)_2$, and (F) $(HL_L)_2(FL_L)_2$, respectively.
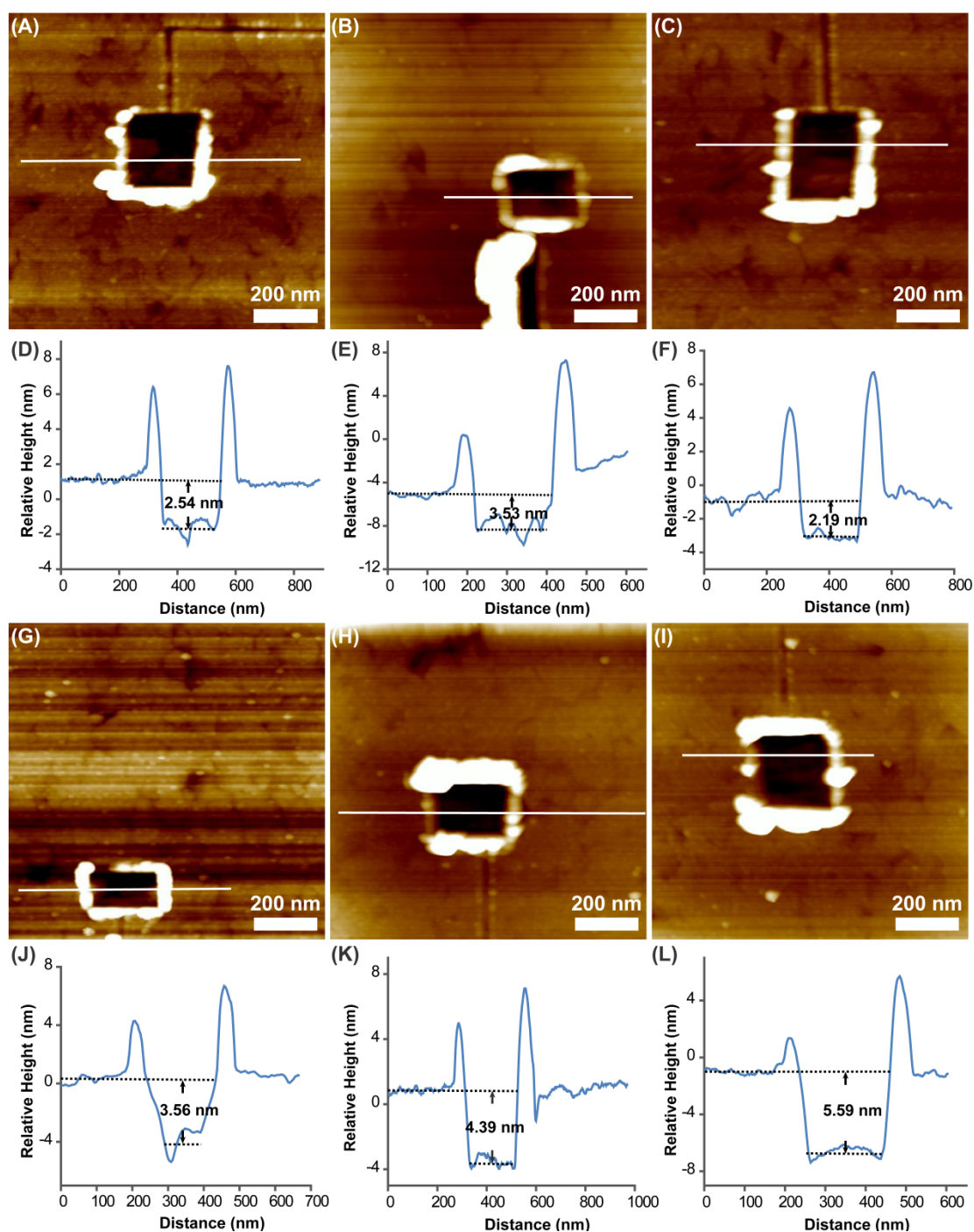
Figure S8. AFM topographic images of (A) CL_SHL_S, (B) $(CL_S)_2(HL_S)_2$, (C) HL_SFL_S, (G) $(HL_S)_2(FL_S)_2$, (H) $(HL_M)_2(FL_M)_2$, and (I) $(HL_L)_2(FL_L)_2$ after nano-shaving using an AFM tip, respectively. (D), (E), (F), (J), (K), and (L) is the corresponding cursor profiles indicated by the line in (A), (B), (C), (G), (H), and (I), respectively. By removing the implanted molecules on the gold surface, the height differences between the shaved region and surrounding areas were measured, which is considered to be the height of the SAMs. The dark squares in each image are the scratched regions.

Molecules removed by the AFM tip aggregate surround the shaved regions and form bright protrusions. From the height difference between the shaved regions and the surrounding SAMs, the thickness of these oligomers are measured, which is consistent with the film thickness as reported previously with similar structures.[1, 2]
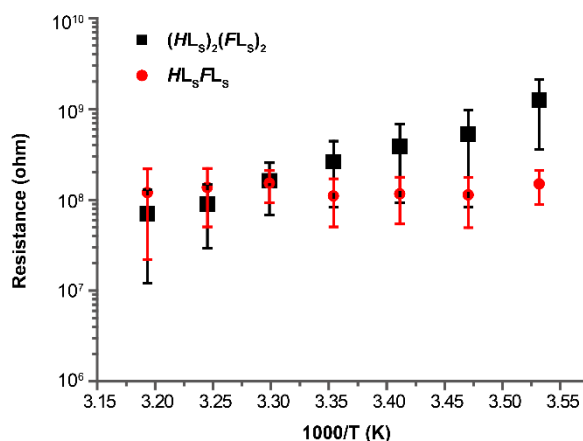

Figure S9. Arrhenius plot for $H\mathrm{L_SF L_S}$ (in red), and $(H\mathrm{L_S})_2(F\mathrm{L_S})_2$ (in black). Each data point is the average differential resistance obtained at six different locations on samples in the range –0.2 to +0.2 V. Error bars, 1 SD.

References：

1.   D. Bu, Y. Xiong, Y. N. Tan, M. Meng, P. J. Low, D. B. Kuang and C. Y. Liu, *Chemical Science*, 2018, **9**, 3438-3450.

2.   D. Bu, Y. Xiong, Y. N. Tan, M. Meng and C. Y. Liu, *Chem. Commun.*, 2018, **54**, 3632-3635.